Hindawi
International Journal of Photoenergy
Volume 2019, Article ID 1486749, 14 pages
https://doi.org/10.1155/2019/1486749

Research Article

Optimum Array Spacing in Grid-Connected Photovoltaic Systems considering Technical and Economic Factors

S. Sánchez-Carbajal and P. M. Rodrigo

Universidad Panamericana, Facultad de Ingeniería, Josemaría Escrivá de Balaguer 101, Aguascalientes 20290, Aguascalientes, Mexico

Correspondence should be addressed to S. Sánchez-Carbajal; santiagoscarbajal@gmail.com

Received 22 August 2018; Revised 15 October 2018; Accepted 12 November 2018; Published 16 January 2019

Academic Editor: Santolo Meo

The performance and economics of grid-connected photovoltaic (PV) systems are affected by the array spacing. Increasing the array spacing implies reducing the impact of shading, but at the same time, it increases the land purchase/preparation costs and the wiring costs. A number of technical and economic factors are involved when selecting an optimum array spacing. Designers of PV plants often set the row-to-row spacing based on simplified rules, losing the opportunity of improving the profitability of their projects. In this paper, a comprehensive methodology for optimizing the array spacing is proposed. It is based on annual shading energy calculations and incorporates a PV energy yield model together with an economic model focused on investment costs. The method is applied to the climatic conditions in Aguascalientes, Mexico, as a case study. A sensitivity analysis allowed the impact of the technical and economic parameters involved on the optimum interrow distance to be quantified. According to the results, the most relevant technical parameters are the module tilt (often considered by the PV designers), the ratio of plant width to plant length, and the module efficiency. The main economic parameters are the land-related costs and the costs per kWp. The comparison of this methodology to a conventional rule based on the winter solstice condition shows differences in the array spacing for the same location when the multiple technical and economic parameters are considered. Therefore, the proposed method will be useful for PV designers to improve the energetic and economic behavior of their systems.

1. Introduction

There are several parameters of photovoltaic (PV) plants that can be easily modified during the early design affecting the profitability of the project. Among them, the interrow spacing plays a significant role. Increasing the array spacing implies higher annual energy output because of the reduced impact of shading, but at the same time, it raises costs of land purchase/preparation and wiring costs. Therefore, methodologies that optimize the array spacing can be developed. However, as a number of technical and economic parameters are involved in the optimization problem, the solution is more complex than those commonly employed in the PV industry. Designers of PV plants are losing the opportunity of improving the profitability of their projects because of the lack of comprehensive methodologies regarding this issue.

The problem of self-shading between rows of collectors has been analyzed in several early studies form the approach of incident energy. These analyses allowed a better understanding of the main design parameters involved in the shading effect and are applicable for both PV and solar thermal fields. An algorithm was proposed for calculating a measurement of the shading efficiency, for stationary collectors and for some cases of sun tracking [1]. From this efficiency value, the designers can set acceptable interrow spacing. In [2], authors calculated the instantaneous shading factor of a field consisting of rows of collectors parallel to the east-west direction and oriented facing the equator, allowing different array widths for the different rows, but no optimization of the row-to-row distance was implemented. The shading effect created by a south-facing vertical pole, inclined pole, vertical collector, and inclined collector over a one-year cycle was

explained in [3]. The objective of this method is to observe the variation of the amount of solar energy received by the collector per unit of area by changing the row-to-row distance of the collectors at any collector tilt. This method was also applied for spacing analysis in Las Vegas, Phoenix, and Albuquerque in [4]. Mathematical optimization techniques were proposed to maximize annual incident energy on a given field, minimize the field area for a given annual incident energy, and maximize the annual incident energy per unit collector area from a given field [5]. These techniques allow simultaneously optimizing collector height and tilt, interrow distances, and number of rows. The results were compared with a simple rule for calculating array spacing proposed by the Israeli Institute of Standards. A more recent contribution proposed a method that calculates the exact shading region on the land generated by each collector over the whole day of winter solstice considering equator-pointed collectors installed on a horizontal land [6]. The interrow distance can be selected to minimize shading based on this shading region.

Specifically, focused on PV systems, there are several studies that go deeper into the subject. A vector-based algorithm was proposed for roofs with a constant tilt different from horizontal and variable collector orientation, which optimizes the row-to-row distance based on a modified winter solstice rule [7]. The algorithm was implemented in the Australian PV Institute Solar Potential Tool [8]. The constrained optimization problem to solve the optimal design of stationary and single axis PV fields was improved by considering the electrical interconnection of the PV modules for achieving maximum yearly output energy from a given field area [9]. Finally, several studies have incorporated economic methodologies in the optimization problem. An analytical hierarchy process was proposed to weight the decision factors and to determine optimum tilt and row distances for flat roofs in cold climates, where capital cost and payback period of the investment are considered [10]. The 21st day of each month was analyzed in terms of shading calculations in this study. A levelized cost of energy (LCOE) approach for PV installations in preexisting building roofs considering the roof tilt and the collector tilt and orientation was also developed [11]. Several cases were analyzed by these authors in order to minimize the LCOE for a specific rooftop.

In spite of the different works reported in the literature, we found several limitations in the reviewed papers. Firstly, most research analyze the incident solar energy on the collector field under shading, but do not deal with the output of the PV system, which is affected by a number of factors, not only irradiance. Secondly, many of the reviewed papers focus on the shading issue in a specific day of the year (generally the winter solstice, in which it is assumed that the shading impact is the greatest) while an annual energy approach would provide more accurate optimization results. Thirdly, while there are some papers that consider economic factors in the optimization of array spacing, they limit the study to specific cases and there is not a general framework that allows the influence of each economic or technical parameter to be assessed.

In this contribution, the optimum array spacing in stationary grid-connected PV systems installed on a horizontal land is analyzed considering the annual energy yield and an economic objective function. The comprehensive PV model, which incorporates the investment costs of the system, allows the impact of different technical and economic parameters to be evaluated. This gives the designers of PV plants a better understanding of the different influencing factors, allowing a better selection of the system components and plant geometry for improving the profitability of their projects. The methodology offers three main novelties with respect to the reviewed literature: first, the economic objective function is exclusively based on system costs, which are easily obtained from the project budget, avoiding the need of financial or other parameters difficult to get; second, the PV model incorporates several technical parameters, such as PV module efficiency and degradation of efficiency with temperature or DC and AC system losses, which allow a more accurate consideration of the electricity output of the system compared to previous authors; third, the model is analytical and easy to implement without the need of the specific software or complex algorithms used by other authors. The proposed methodology is applied to the typical climatic conditions in Aguascalientes, Mexico. Data measured over 10 years at 10-minute intervals is used for generating the typical meteorological year. However, the comprehensive methodology can be easily applied to other locations with available climatic data.

2. Materials and Methods

2.1. Meteorological Data. This study is based on records of global horizontal irradiance (G_{hor}) and ambient temperature (T_{amb}) taken from December 2005 to April 2015 at 10-minute intervals in a meteorological station located near the center of Aguascalientes city (21.9°N, −102.3°E). This big volume of data was processed to get the typical meteorological year of Aguascalientes. The procedure consisted in calculating the monthly global horizontal irradiation for each month in the dataset and the monthly average global horizontal irradiation for each month (January, February, etc.); after that, we searched the month in the dataset that better matches the calculated average monthly global horizontal irradiation. This month is selected as one of the months of the typical meteorological year. As a result, 12 real months from different years are selected to represent the typical year.

In order to be confident that the generated meteorological year represents adequately the typical climatic conditions of the location, we validated the annual histograms of G_{hor} and T_{amb} by comparing the generated typical year to the 10 years' dataset. These histograms are shown in Figure 1. As can be seen, there is a good similarity between the histograms of the typical year and those of the 10 years' dataset. Thus, we can use the generated typical year as representative of the average climate in Aguascalientes. Actually, this is a remarkable aspect of the current contribution because we used for every simulation a typical year at 10-minute intervals, while many authors perform these kinds of calculations based on hourly values, often generated from monthly average values

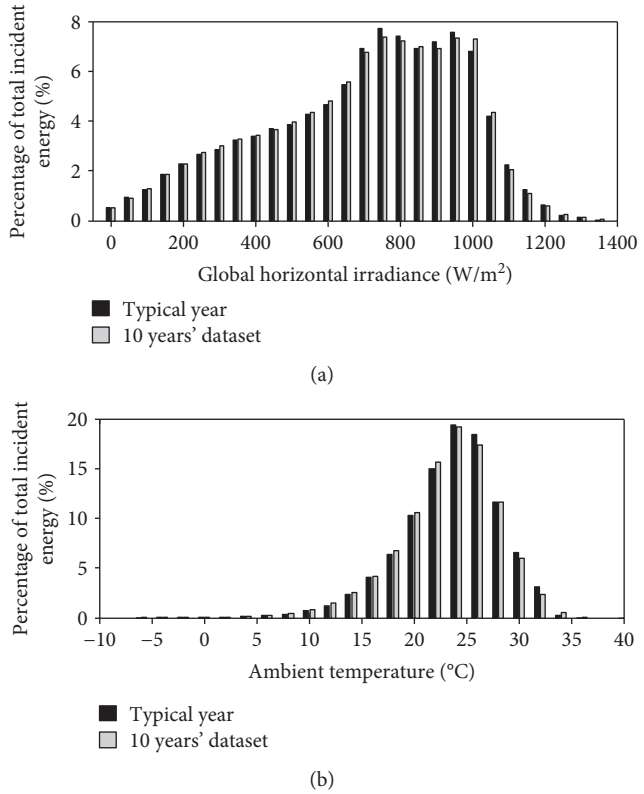

Figure 1: Comparison of annual histograms of global horizontal irradiance (a) and ambient temperature (b) between the generated typical year and the 10 years' dataset.

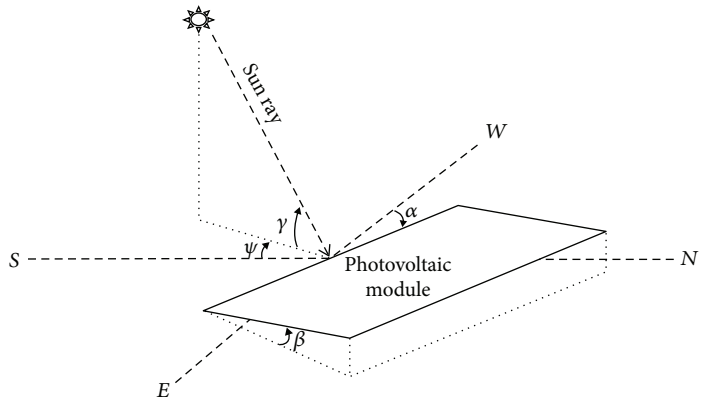

Figure 2: Angles that define the position of the PV arrays and the sun position.

taken from online meteorological databases. Therefore, the presented methodology is necessarily more accurate than it is usual in the literature.

The radiation inputs of the PV energy yield model are the diffuse horizontal (D_{hor}) and the direct horizontal (B_{hor}) irradiances. As these magnitudes are not directly provided by the meteorological dataset, they were calculated by using Iqbal's correlation between the diffuse fraction and the clearness index [12]. The details of this calculation can be read in a previous contribution [13].

2.2. Irradiance Calculations considering Array Shading. The basic angles that determine the position of the PV arrays and the sun are defined in Figure 2. For positioning the PV arrays, the orientation (α) and tilt (β) angles are shown ($\alpha = 0^\circ$ means PV modules facing the equator). For positioning the sun, the azimuth (ψ) and the elevation (γ) are needed ($\psi = 0^\circ$ means sun coming from the equator).

In order to consider self-shading between rows of PV modules, the magnitudes shown in Figure 3 are used. The free distance between two adjacent rows is named as d. This distance together with the β tilt angle and the l collector height defines the spacing between parallel rows. Note that the collector height can be obtained with one or several lines of coplanar PV modules; i.e., it does not necessarily equal the height of one PV module. The row spacing is then $l \bullet \cos\ \beta + d$

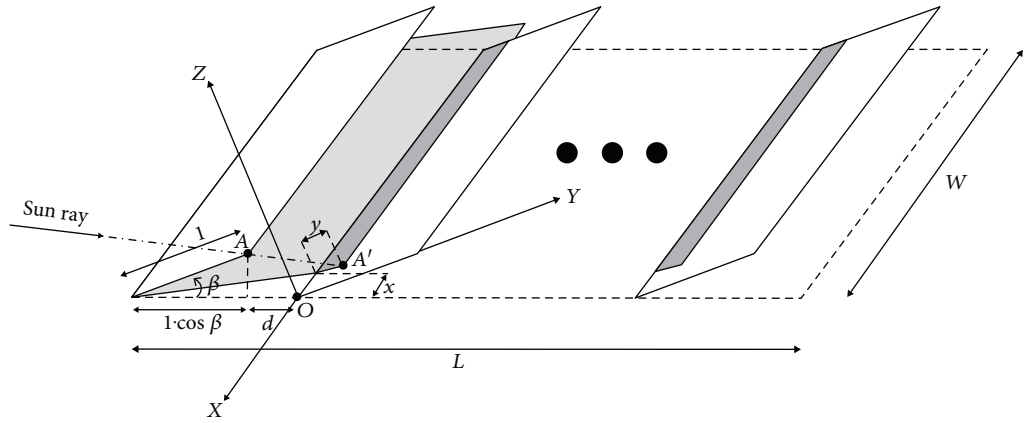

Figure 3: Geometry for calculating self-shading between parallel rows of PV modules.

, as shown in the figure. L and W are the length and width of the plant, respectively.

For obtaining the shaded rectangle on a row caused by a previous row, the coordinates of the A' point on the OXYZ reference are needed. The A' point is the intersection of the line that matches the direction of the sun ray and contains the A point (one of the corners of the previous row) with the plain of the shaded row. This intersection can be mathematically expressed as

$$\begin{bmatrix} x \\ y \\ 0 \end{bmatrix} = \begin{bmatrix} 0 \\ l \\ 0 \end{bmatrix} - R_2 \begin{bmatrix} 0 \\ l\cos\beta + d \\ 0 \end{bmatrix} + \lambda R_2 R_1 \begin{bmatrix} 0 \\ \cos\gamma \\ -\sin\gamma \end{bmatrix}, \tag{1}$$

where R_1 and R_2 are the following rotation matrices:

$$R_1 = \begin{bmatrix} \cos(\psi-\alpha) & \sin(\psi-\alpha) & 0 \\ -\sin(\psi-\alpha) & \cos(\psi-\alpha) & 0 \\ 0 & 0 & 1 \end{bmatrix}, \quad R_2 = \begin{bmatrix} 1 & 0 & 0 \\ 0 & \cos\beta & \sin\beta \\ 0 & -\sin\beta & \cos\beta \end{bmatrix}. \tag{2}$$

The three expressions in Eq. (1) contain three unknowns: x, y, and λ. Clearing the third equation allows the λ expression to be determined:

$$\lambda = \frac{(l\cos\beta + d)/\cos\gamma}{\cos(\psi-\alpha) + (\tan\gamma/\tan\beta)}. \tag{3}$$

The sign of the λ parameter indicates if the sun comes in front of the PV modules ($\lambda > 0$) or behind them ($\lambda \le 0$). The condition $\lambda > 0$ is equivalent to $\cos(\psi-\alpha) + (\tan\gamma/\tan\beta) > 0$. Clearing the first and second equations in Eq. (1) allows the expressions for x and y to be determined in a similar way.

In this study, normalized notation is used to perform an analysis as general as possible. The following variables normalized to the l collector height will then be used: d/l, W/l, x/l, and y/l. The aim of the shading analysis is to get two shading factors: f_{s1} (shading factor of the first row of the plant) and f_{s2} (shading factor of the second and subsequent rows of the plant). A shading factor represents the ratio of the shaded area to the total collector area of a row. Using the normalized notation, these shading factors can be calculated by the following algorithm:

$$\lambda_0 = \cos(\psi-\alpha) + \frac{\tan\gamma}{\tan\beta}$$

$$If\ \lambda_0 \le 0\ then\ f_{s1} = f_{s2} = 1$$

$$Else \begin{cases} f_{s1} = 0 \\ x/l = (\cos\beta + d/l)\dfrac{\sin(\psi-\alpha)}{\lambda_0} \\ y/l = 1 - (\cos\beta + d/l)\dfrac{\tan\gamma}{\lambda_0 \sin\beta} \\ If\ y/l \le 0\ then\ f_{s2} = 0 \\ Else if\ (x/l \le -W/l)\,\mathrm{OR}\,(x/l \ge -W/l)\ then\ f_{s2} = 0 \\ Else\ f_{s2} = \left(1 - \dfrac{|x/l|}{W/l}\right) y/l \end{cases}. \tag{4}$$

The shading factors will be used to correct the direct irradiance incident on the rows of PV modules. The diffuse and albedo irradiances must be calculated from the horizontal diffuse and the horizontal global irradiances, respectively, by applying the so-called "view factors to sky" corrections. We can distinguish two view factors to sky: F_{sky1} (that of the first row of the plant) and F_{sky2} (that of the second and subsequent rows). These can be calculated following the expressions proposed in [14]:

$$F_{\text{sky1}} = \frac{1+\cos\beta}{2},$$
$$F_{\text{sky2}} = \frac{1+\cos\beta + d/l - \sqrt{\sin^2\beta + (d/l)^2}}{2}. \quad (5)$$

From these view factors, the diffuse (D_i) and albedo (A_i) irradiances on the rows of PV modules are calculated (note that we distinguish between the first row, subscript "1," and the second and subsequent rows, subscript "2"):

$$D_1 = F_{\text{sky1}} D_{\text{hor}},$$
$$D_2 = F_{\text{sky2}} D_{\text{hor}},$$
$$A_1 = \rho G_{\text{hor}}\left(1 - F_{\text{sky1}}\right), \quad (6)$$
$$A_2 = \rho G_{\text{hor}}\left(1 - F_{\text{sky2}}\right),$$

where ρ is the albedo coefficient. It is set to 0.2 in the present study corresponding to an urban environment. The direct irradiance incident on the plane of the PV arrays (prior to the shading correction), B, can be calculated from the direct horizontal irradiance, B_{hor}, by

$$B = B_{\text{hor}} \frac{\cos\theta_n}{\sin\gamma}, \quad (7)$$

where θ_n is the angle of incidence of the rays of the sun as compared with the normal of the PV modules, which is obtained through trigonometric relations [15]. Finally, the average global irradiances incident on the rows of PV modules considering the shaded areas, G_{s1} and G_{s2}, are calculated by

$$G_{s1} = (1 - f_{s1})B + D_1 + A_1,$$
$$G_{s2} = (1 - f_{s2})B + D_2 + A_2. \quad (8)$$

The average global irradiance for the whole plant (G_s) can be obtained by considering the number of rows that comprise it (N_r):

$$G_s = \frac{G_{s1} + (N_r - 1)G_{s2}}{N_r}, \quad (9)$$

where N_r can be expressed as a function of the normalized magnitudes that define the PV plant:

$$N_r = \frac{W/l}{W/L(\cos\beta + d/l)}, \quad (10)$$

W/L is the plant aspect ratio or the ratio of plant width to plant length. With this procedure, G_s can be obtained at each time interval. The calculation of the annual global irradiation incident on the PV generator in kWh/(m^2 year), H_s, can be done by an annual summation as

$$H_s = \frac{\sum_i G_{si} \cdot \Delta t}{1,000}. \quad (11)$$

Δt is the time step for the irradiance calculations (1/6 hr in this study).

2.3. Energy Yield Model. The annual energy yield of the PV system in kWh/kWp (Y) can be calculated from the annual global irradiation by considering the different types of losses that exist in the system [16]:

$$Y = H_s(1 - L_T)(1 - L_{DC})\eta_{\text{inv}}(1 - L_{AC}), \quad (12)$$

where L_T represents the annual thermal losses, L_{DC} is the coefficient of losses in the DC side, η_{inv} is the annual inverter efficiency, and L_{AC} is the coefficient of losses in the AC side. L_T and η_{inv} are calculated in detail as a function of the operating conditions, while L_{DC} and L_{AC} are expressed as annual coefficients. The sensitivity analysis in Section 5 will show the influence of these coefficients, which can vary from one system to another, on the optimum array spacing.

The calculation of the annual thermal losses is done based on the temperature coefficient of maximum power of the PV module (γ_{mod}) and on annual summations as

$$L_T = \gamma_{\text{mod}} \frac{\sum_i G_{si}(T_{ci} - T_c^*)}{\sum_i G_{si}}, \quad (13)$$

where T_{ci} are the values of cell temperature at each instant and T_c^* is the cell temperature at standard test conditions (25°C). The cell temperature values are calculated according to the standard PV method based on the nominal operating cell temperature (NOCT) coefficient [17]:

$$T_{ci} = T_{\text{amb},i} + \frac{G_{si}}{800}(\text{NOCT} - 20). \quad (14)$$

NOCT is set in this study to 45°C corresponding to normal values found in the datasheets of commercial PV modules.

The calculation of the annual inverter efficiency is done by weighting the instantaneous values of inverter efficiency ($\eta_{\text{inv},i}$) with the incident global irradiance:

$$\eta_{\text{inv}} = \frac{\sum_i G_{si}\eta_{\text{inv},i}}{\sum_i G_{si}}, \quad (15)$$

where $\eta_{\text{inv},i}$ can be expressed as a function of the inverter loss coefficients (L_0, L_1, and L_2) and the maximum power of the PV array normalized to the inverter nominal power ($p_{\text{in},i}$) as [18, 19]

$$\eta_{\text{inv},i} = 1 - \frac{L_0 + L_1 p_{\text{in},i} + L_2 p_{\text{in},i}^2}{p_{\text{in},i}}. \quad (16)$$

The inverter loss coefficients are set in this study to $L_0 = 0.0048$, $L_1 = 0.0159$, and $L_2 = 0.0144$ according to typical values of medium-efficiency inverters obtained from a

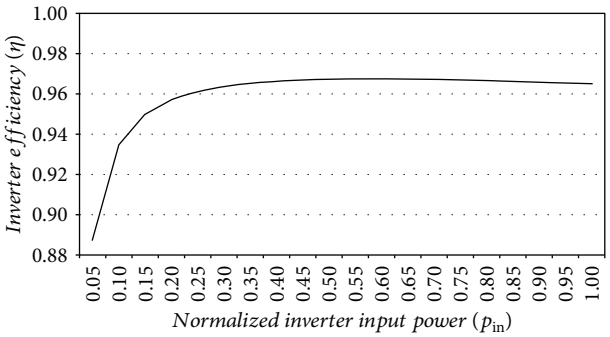

Figure 4: Efficiency curve of typical medium-efficiency inverter as a function of the normalized inverter input power.

survey of 80 commercial inverter datasheets published in [20]. The efficiency curve of this typical inverter is shown in Figure 4. The $p_{in,i}$ values are calculated considering the DC-to-AC sizing ratio of the inverter ($r_{DC/AC}$) or ratio of the PV array peak power to the inverter nominal power:

$$p_{in,i} = r_{DC/AC}\frac{G_{si}}{1000}[1-\gamma_{mod}(T_{ci}-T_c^*)](1-L_{DC}). \quad (17)$$

$r_{DC/AC}$ is set to 1.2 according to typical inverter sizing values used in Aguascalientes for improving the annual inverter efficiency and lowering the cost of inverters [21]. It must be highlighted that Eq. (16) expresses the instantaneous inverter efficiency under normal operating conditions. However, in the periods of high irradiance, the inverter can limit the output power to the inverter nominal power in order to not exceed this maximum output power. When this condition verifies, the inverter efficiency is simply expressed as

$$\eta_{inv,i} = \frac{1}{p_{in,i}}. \quad (18)$$

2.4. Economic Objective Function. The proposed methodology is aimed at maximizing the annual energy generated by the PV system per unit investment cost; i.e., the economic objective function (Γ) is

$$\Gamma = Y/C_{kWp,tot}, \quad (19)$$

where $C_{kWp,tot}$ is the total investment cost per installed kWp. In this way, the objective of this analysis is to maximize Γ. $C_{kWp,tot}$ needs to be broken down as a sum of three costs:

$$C_{kWp,tot} = C_{kWp} + C_{kWp,str} + C_{kWp,land}, \quad (20)$$

where $C_{kWp,str}$ represents the cost of structure used to support the PV modules per installed kWp, $C_{kWp,land}$ represents the cost associated to land area per installed kWp, and C_{kWp} represents the rest of investment costs per installed kWp. The land related cost $C_{kWp,land}$ includes cost of land purchase/preparation, together with wiring costs. Equation (20) can also be expressed as

$$C_{kWp,tot} = C_{kWp} + C_{m2str}\cdot A_{str\,per\,kWp} + C_{m2land}\cdot A_{land\,per\,kWp}. \quad (21)$$

C_{m2str} and C_{m2land} are the cost per m^2 of supporting structure and land, respectively, $A_{str\,per\,kWp}$ the structure area per installed kWp, and $A_{land\,per\,kWp}$ the land area per installed kWp. The last two areas can be expressed as a function of the standard efficiency of the PV modules (η_{mod}) taking into account that

$$\eta_{mod} = \frac{1}{A_{str\,per\,kWp}} = \frac{1}{GCR\cdot A_{land\,per\,kWp}}, \quad (22)$$

where GCR is the ground coverage ratio of the PV plant or ratio of the PV array area to the land area. Therefore, the final expression for the economic objective function is

$$\Gamma = \frac{Y}{C_{kWp} + C_{m2str}/\eta_{mod} + C_{m2land}/(GCR\cdot\eta_{mod})}. \quad (23)$$

Note that *GCR* can be easily calculated as

$$GCR = \frac{1}{\cos\beta + d/l}. \quad (24)$$

Thus, an economic objective function has been developed, which depends on many technical and economic parameters of the PV plant.

2.5. Optimization Algorithm. The optimization of the array spacing consists on finding the optimum *d*/*l* that maximizes Γ for a set of given technical and economic parameters. This optimization problem can be successfully solved with the Nelder-Mead simplex algorithm as described in [22]. The algorithm is implemented in the standard *fminsearch* function of Matlab®. It uses a simplex of $n+1$ points for n -dimensional vectors x. First, it makes a simplex around the initial guess x_0 by adding 5% of each component $x_0(i)$ to x_0. These n vectors are used as elements of the simplex in addition to x_0. Then, the algorithm modifies the simplex repeatedly according to a procedure that can be summarized as

(1) $x(i)$ $i = 1,\ldots,n+1$ represents the current simplex

(2) Order the points in the simplex from lowest function value $f(x(1))$ to highest $f(x(n+1))$. At each step in the iteration, the algorithm discards the current worst point $x(n+1)$, and accepts another point into the simplex

(3) Generate the r reflected point and calculate $f(r)$:

$$r = 2\sum_{i=1}^{n}\frac{x(i)}{n} - x(n+1) \quad (25)$$

(4) If $f(x(1)) \le f(r) < f(x(n))$, accept r and terminate this iteration

(5) If $f(r) < f(x(1))$, generate the s expansion point and calculate $f(s)$:

$$s = m + 2(m - x(n+1)) \quad (26)$$

If $f(s) < f(r)$, accept x and terminate the iteration. Otherwise, accept r and terminate the iteration.

(6) If $f(r) \geq f(x(n))$, perform a contraction between m and the better of $x(n+1)$ and r:

If r is better than $x(n+1)$, calculate $c = m + (r\text{-}m)/2$ and calculate $f(c)$. If $f(c) < f(r)$, accept c and terminate the iteration. Otherwise, continue with Step 7.

If r is equal or worse than $x(n+1)$, calculate $cc = m + (x(n+1)\text{-}m)/2$ and calculate $f(cc)$. If $f(cc) < f(x(n+1))$, accept cc and terminate the iteration. Otherwise, continue with Step 7.

(7) Calculate the n points:

$$v(i) = x(1) + (x(i) - x(1))/2 \quad i = 2, \ldots, n+1 \quad (27)$$

Also calculate $f(v(i))$. The simplex at the next iteration is $x(1), v(2), \ldots, v(n+1)$.

3. Model Parameterization

In the present paper, a case base composed of a set of values for the input parameters is stablished. This case base represents a typical medium-sized PV plant. However, the behavior of the optimization model has been analyzed by allowing the variation of each parameter within a minimum and a maximum value in order to consider different possibilities both technical and economical for the PV plant configuration. The case base, minimum, and maximum values of each model parameter as considered in the current study are shown in Table 1.

The PV module orientation (α) in the case base is considered as equator-facing, while in the other cases a difference of -15° and 15° is considered to fit the orientation of the rooftop or the land available in which the PV modules are placed.

For the PV module tilt angle (β), the case base is set to 20°. The reason for this is that the mounting structures that are sold in Aguascalientes are often designed with this angle, similar to the site latitude. Nevertheless, different values are considered for the module tilt, 10° for the minimum because in some cases more power is needed to be placed on the limited space and 30° for the maximum because in some cases the space is narrow and the PV modules need to be placed this way.

For the normalized row width (W/l), the case base sets the value to 20 meaning that we would have 40 PV modules of 72 cells (2 meters of collector height and 1 meter of collector width) in one row, which can be a commonly used value for a medium-sized PV installation. Meanwhile, the minimum case takes the value of 7 and in the maximum case the value is 50 in order to adapt to different row sizes.

Table 1: Analyzed values of the input parameters: minimum value, case base value, and maximum value.

Parameter	Minimum value	Case base value	Maximum value	Unit
α	−15	0	15	$^\circ$
β	10	20	30	$^\circ$
W/l	7	20	50	—
W/L	0.2	1	10	—
γ_{mod}	0.0032	0.0040	0.0048	$^\circ C^{-1}$
L_{DC}	0.07	0.1	0.2	—
L_{AC}	0.01	0.02	0.05	—
η_{mod}	0.12	0.17	0.20	—
C_{kWp}	900	1100	1400	USD/kWp
C_{m2str}	22	25	28	USD/m^2
C_{m2land}	6	10	33	USD/m^2

For the plant aspect ratio (W/L), the case base is set to 1 meaning that the available land is squared. The minimum case of 0.2 takes into account that the available land has a small width compared to its length while the maximum case of 10 means that the available land has a greater width compared to its length.

For the temperature coefficient of the PV module (γ_{mod}), the case base considers $0.0040^\circ C^{-1}$, which is a typical value for commercial crystalline silicon PV modules. For the minimum case, the value is $0.0032^\circ C^{-1}$ considering thin film PV modules, while for the maximum case the value is set to $0.0048^\circ C^{-1}$ meaning that the silicon used to manufacture the PV cells and the overall quality of the PV module is not top quality.

For the DC loss coefficient (L_{DC}), the case base is set to 0.1 meaning that 10% of the DC power is lost considering that the local regulation involving power loss in wires is successfully fulfilled and the soiling losses are kept to an acceptable level. In the minimum case, the value is set to 0.07 meaning that a strict maintenance policy is applied for mitigating soiling losses. On the other hand, for the maximum case, the value of 0.2 means that the wires used in the installation barely cover the local regulation requirements and the maintenance policy is barely applied or is nonexistent.

For the AC loss coefficient (L_{AC}), the case base holds the value of 0.02 meaning that the local regulation involving power loss in wires is successfully fulfilled and there is not a power transformer. For the minimum case, the value is 0.01 considering that the wire loss is greatly mitigated by selecting a higher wire gauge than the necessary. Meanwhile, in the maximum case, a value of 0.05 is set considering that the wire gauge is barely covering the requirements of the local regulation and/or the power transformer is installed.

For the photovoltaic module efficiency (η_{mod}), the case base is set to 0.17 meaning that the PV module used in the installation is a crystalline silicon module made from regular quality elements. In the minimum case, the value of 0.12 corresponds to low-efficiency thin film PV modules. For the

maximum case, the value is set to 0.20 meaning that the module is made of monocrystalline cells and is manufactured from high-quality components.

For the peak power-related costs (C_{kWp}), the case base is set to 1100 USD/kWp meaning that the installation is medium-sized and considering the local prizes for the region of Aguascalientes. For the minimum case, the value is set to 900 USD/kWp corresponding to a utility-scale installation, while for the maximum case the value is 1400 USD/kWp corresponding to a small-sized installation.

For the structure-related cost (C_{m2str}), the case base is set to 25 USD/m^2 corresponding to a typical aluminum structure designed for rooftop applications. For the minimum case, the value is 22 USD/m^2 considering a reduction in the material cost due to scale economics. For the maximum case, a value of 28 USD/m^2 is considered, considering a structure made of cold rolled iron protected by an epoxy paint and suitable for land application. This structure needs some infrastructure to be done like foundations made from iron and cement.

For the land-related cost (C_{m2land}), the case base is set to 10 USD/m^2 considering that the land is far from the city and it is for agricultural use making the price per square meter more affordable. For the minimum case, 6 USD/m^2, it is considered that the land is pre-owned and the only expense would be the acquisition of wires, the making of the ditch, and the registers and the hand work of putting the wires in the ducts and registers. For the maximum case, the value is set to 33 USD/m^2 considering the price per square meter of an industrial polygon near the city.

4. Results

The proposed method allows the normalized free distance between rows (d/l) to be optimized by considering technical and economic parameters of the PV plant. The optimization process is illustrated in Figure 5. In this figure, the energy yield and the economic objective function are plotted versus d/l for three different scenarios. In the top graph, the cost per unit land area (C_{m2land}) is set to 6, 10, and 33 USD/m^2; in the middle graph, the plant aspect ratio (ratio of plant width to plant length, W/L) is set to 1 and 10. In the bottom graph, the PV module efficiency (η_{mod}) is set to 0.12, 0.17, and 0.20. The rest of the model parameters are kept to the values of the case base. This way, the influence of an economic parameter (C_{m2land}), a geometric parameter (W/L), and a technical parameter (η_{mod}) on the optimum d/l can be analyzed.

With respect to Figure 5 top, it can be seen that changing C_{m2land} does not influence the energy yield. However, it modifies the economic objective function; i.e., the objective function decreases with increasing land-related costs for the same d/l distance. The optimum d/l distance is also marked on the graph with a red circle. As can be observed, increasing the land-related costs implies a decrease on the optimum d/l; i.e., the ground covering ratio should be reduced if the land-related costs increase to optimize the economic profitability of the PV plant.

In Figure 5 middle, two values of the plant aspect ratio (1 and 10) are analyzed. $W/L = 1$ represents a squared plant while $W/L = 10$ represents a rectangular plant with wider rows than the plant length. In this case, the value of W/L does influence the energy yield because of the relative importance of the first row of the PV plant, which is the most favorable from the point of view of energy generation. In this way, a plant with $W/L = 10$ exhibits a better energy yield than a plant with $W/L = 1$, as can be seen in the graph. The objective function also grows with increasing W/L because the energy yield is in the numerator of this function. The optimum d/l displaces to the left with increasing W/L. This means that having a greater plant aspect ratio ($W/L = 10$) allows the ground cover ratio to be reduced because we can sacrifice a little of energy yield to a have a lesser PV plant cost due to a smaller area usage.

When analyzing the bottomside of Figure 5, it can be seen that the energy yield is not affected by the PV module efficiency. However, it modifies the economic objective function, i.e., the economic function increases as the PV module efficiency increases for the same d/l distance. This is because a high-efficiency PV module would imply lower costs of structure and lower land-related costs. As can be observed, by having a greater module efficiency, the ground coverage ratio can be decreased because it is more important to take benefit of the increased energy yield (due to lower impact of shading) than to reduce the land-associated costs.

Designers of PV plants often set the array spacing based on a winter solstice rule. This rule is usually employed in order to guarantee that in the winter solstice, which is the day with larger impact of shading, the PV modules are not shaded between 10 : 00 a.m. and 2 : 00 p.m. solar time. Results of a comparison between the array spacing obtained with the winter solstice rule and the optimum obtained with the proposed method are shown in Figure 6. In this figure, the optimum d/l is plotted versus the PV module orientation, which is varied between −15° and 15°. The graph on the left corresponds to a fixed PV module tilt of 20° while the graph on the right corresponds to a fixed PV module tilt of 30°. Each graph compares the winter solstice rule to the proposed method considering three different values of the land-related costs ($C_{m2land} = 6$, 10, and 33 USD/m^2). The figure shows that the proposed method is significantly affected by the land-related costs; i.e., the optimum d/l clearly decreases as the land-related costs increase. As can be seen, the winter solstice rule is not able to adapt the array spacing to the economic parameters of the PV plant. In addition, the optimum array spacing can differ from that calculated with this rule, especially for highly expensive land. Therefore, the widely used winter solstice rule does not necessarily lead to an optimum array spacing from the point of view of the economic profitability of the project. This highlights the interest of considering technical and economic parameters when optimizing the array spacing and the usefulness of the proposed methodology.

5. Sensitivity Analysis

The main results of a sensitivity analysis on the influence of technical and economic parameters on the optimum array spacing are presented in Table 2. The values in this table were

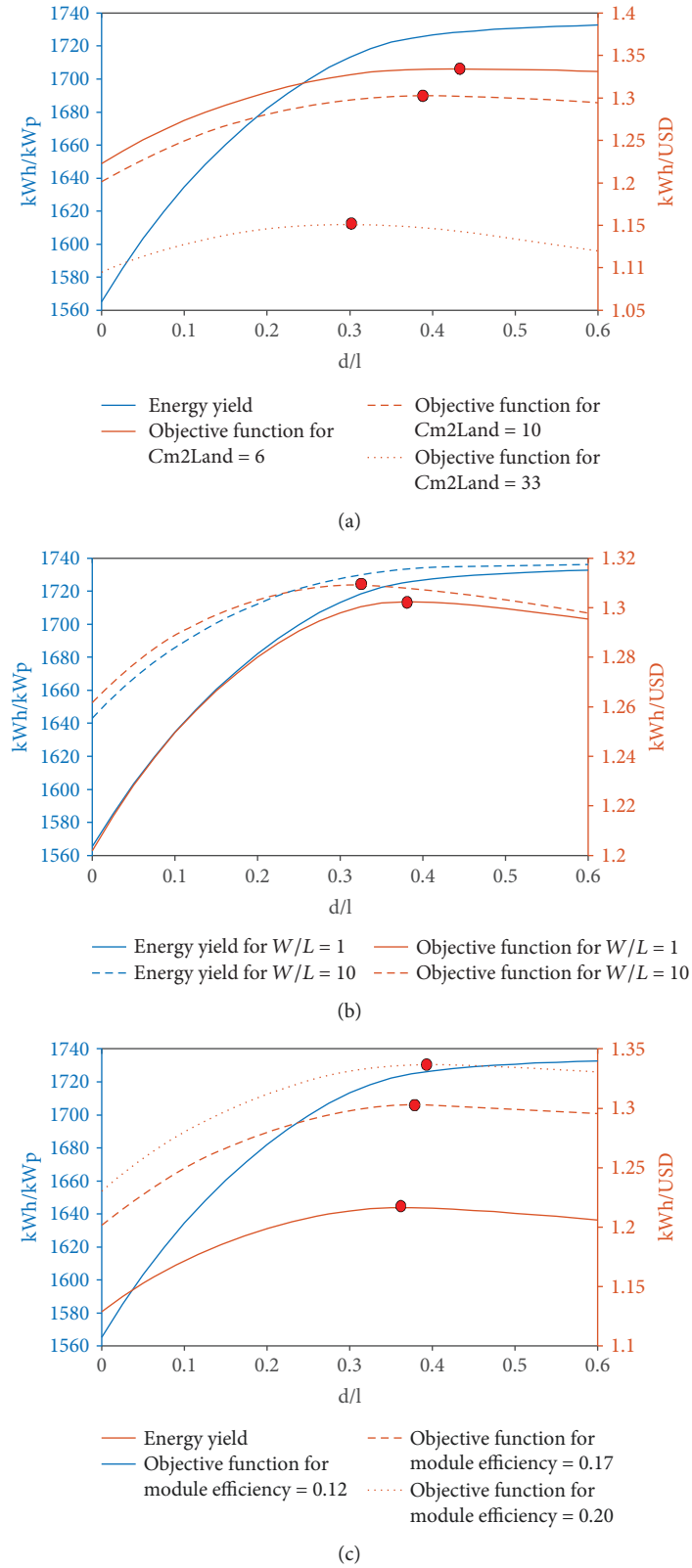

FIGURE 5: Energy yield and economic objective function vs the normalized free distance between rows (d/l): (a) for variable cost per unit land area (C_{m2land}); (b) for the variable plant aspect ratio (W/L); (c) for variable PV module efficiency (η_{mod}).

obtained by changing each influencing parameter within the minimum and maximum values specified in Table 1, while keeping the rest of the model parameters with the assigned value in the case base. The calculated minimum and maximum optimum d/l are reported in the table, as well as the percentage of variation of the optimum d/l with respect to

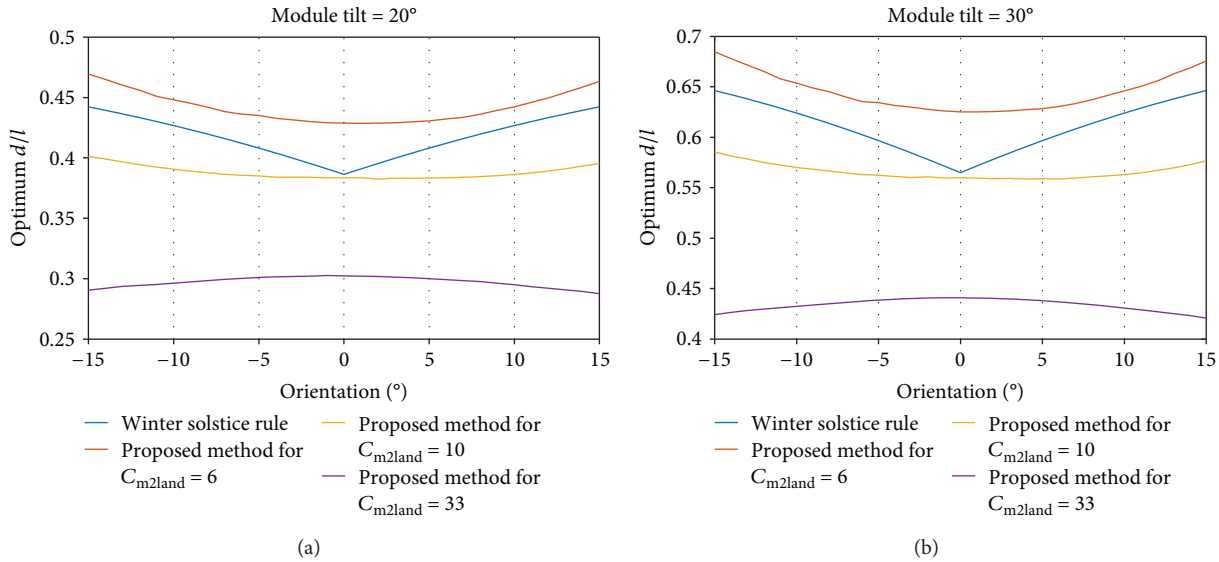

Figure 6: Optimum d/l versus module orientation considering the winter solstice rule and the proposed method with variable land-related cost: (a) for PV module tilt = 20°; (b) for PV module tilt = 30°.

Table 2: Sensitivity analysis of the technical and economic factors influencing the array spacing. Minimum and maximum optimum d/l for each model parameter according to the defined ranges of values, and percentages of variation with optimum d/l ($\Delta d/l$) with respect to the case base ($d/l = 0.383$).

Parameter	d/l opt.min.	d/l opt.max.	$\Delta d/l$ (%)
β	0.196	0.560	94.89
C_{m2land}	0.302	0.429	32.98
W/L	0.330	0.388	15.14
η_{mod}	0.362	0.395	8.45
C_{kWp}	0.370	0.401	7.94
W/l	0.370	0.388	4.76
α	0.383	0.401	4.72
C_{m2str}	0.382	0.385	0.57
L_{DC}	0.382	0.384	0.49
γ_{mod}	0.383	0.384	0.10
L_{AC}	0.384	0.384	0.00

the case base. The reference d/l for the case base is 0.383 in Aguascalientes. The different parameters are sorted according to the optimum percentage variation of d/l, from the most influencing to the least influencing. In this way, the table allows the more significant parameters to be noticed.

As can be seen, the most influencing parameter is the PV module tilt with 94.89% of influence on d/l. This parameter is widely used in the methods for calculating the array spacing in the literature. However, most of these methods do not consider other relevant parameters as in the case of the proposed method. The second influencing parameter is the land-related cost with 32.98% of influence. This is an important economic factor because increasing the land-related costs implies reducing the array spacing. The plant aspect ratio also shows an appreciable influence of 15.14% because of the different impact of the first row of PV modules which is the most favorable for energy production. The efficiency of the PV modules and the peak power-related cost show similar levels of influence with 8.45% and 7.94%, respectively. Also, below them, the normalized plant width and the PV module orientation show 4.76% and 4.72%, respectively. The rest of the model parameters have shown a very small influence, lower than 0.6%.

The behavior of the optimization model with respect to changes in the parameter values has been analyzed in detail. The results for the six parameters with highest influence on the array spacing (β, C_{m2land}, W/L, η_{mod}, C_{kWp}, and W/l) are summarized in Figure 7. As can be observed, the optimum d/l shows an approximate linear behavior for three of these parameters (β, η_{mod}, and C_{kWp}) while for the other three, the behavior is clearly nonlinear. The optimum d/l increases with the parameter value in all cases except for C_{m2land} and W/L. The graphs also show the influence of each parameter on the objective function which gives an idea of the influence of each parameter on the economics of the system. The change in every parameter implies a monotonous increase or decrease of the economic objective function except in the case of the β parameter in which it exhibits a maximum within the range of analyzed values. This maximum corresponds to the optimum tilt of PV modules in Aguascalientes according to the proposed model.

Taking into account the sensitivity analysis, it is worth recommending to the designers of PV plants to incorporate technical and economic parameters in the array spacing calculation. The main technical factors that should be considered are the PV module tilt (which is widely used in these kinds of calculations), the plant aspect ratio, the PV module efficiency, the normalized row width, and the PV module orientation. The main economic factors are the land-related costs and the peak power-related costs. The use of a methodology such as the one proposed in this paper can help in these

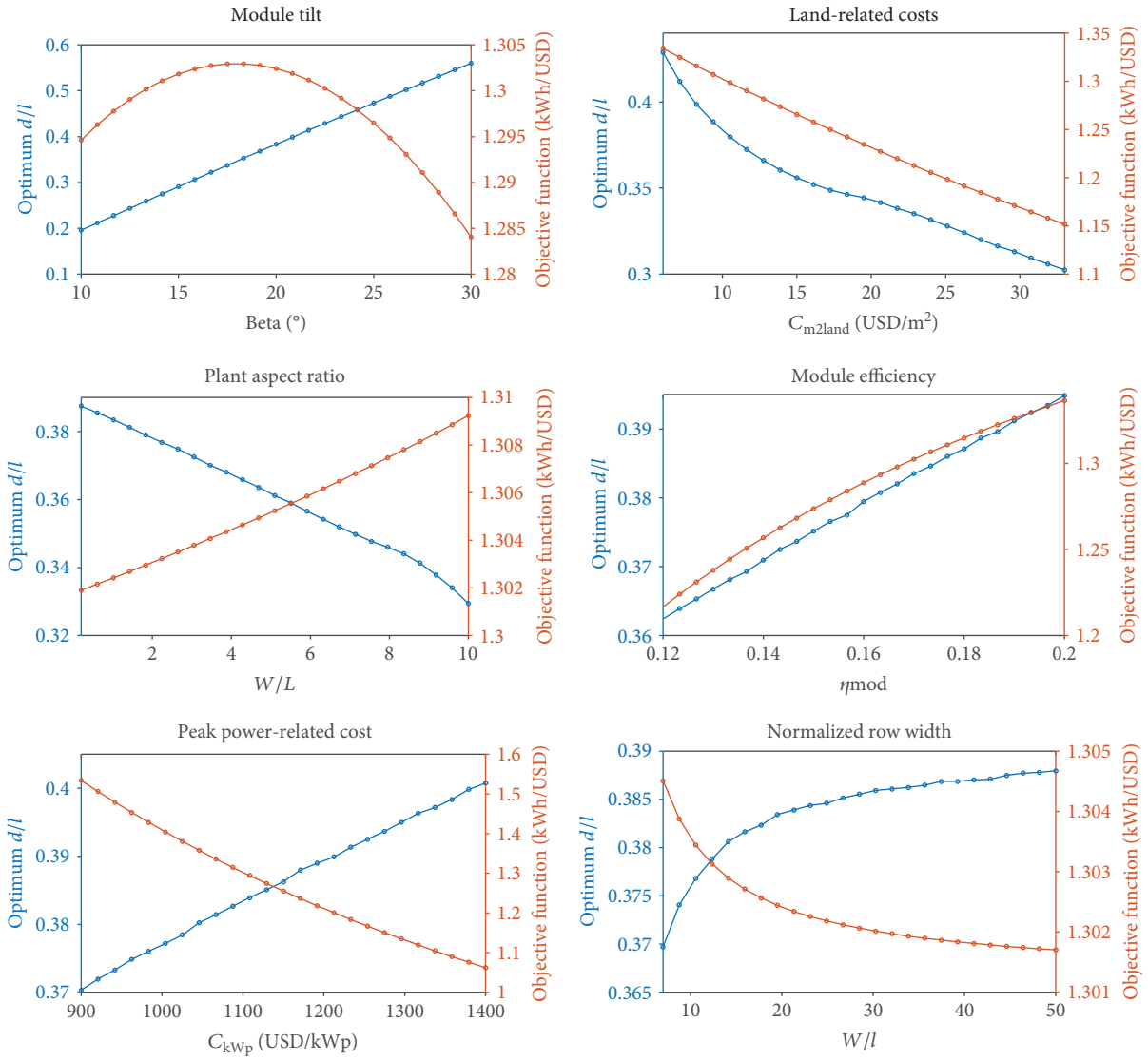

Figure 7: Variation of optimum d/l and objective function for the six parameters with the highest influence on the array spacing.

calculations and hence can help to improve the profitability of the PV projects by optimizing the array spacing.

6. Example of Application

In this section, an example of application of the proposed methodology is presented based on a real PV project that has not yet been implemented. The project is located at Aguascalientes so that the same meteorological data used in the previous sections can be applied. The land must be purchased at 4 USD/m^2. The PV plant consists of 5 mounting structures made from galvanized steel, each one holding 80 PV modules in an arrangement of 4 vertical lines of 20 modules per line (Figure 8). The structures are south-oriented 20° tilted, and the land is horizontal. Renesola Virtus II JC260M-24/Bb polycrystalline silicon modules are used, with 260 Wp per module and a 16.0% module efficiency. The system uses 5 SMA STP17000TL three-phase PV inverters with a nominal capacity of 17,000 W per inverter, each one connected to the 80 PV modules of each mounting structure. In this way, the plant DC-to-AC sizing ratio is 1.22 according to the typical designs of Aguascalientes. A 110 kVA power transformer is installed because the operating voltage of the inverter (230/400 V) differs from the grid voltage (127/220 V). The rectangular available land is 32.8 m × 26.0 m. The information required to run the optimization methodology is shown in Table 3. As can be seen, this information is familiar for the designers of PV plants.

The input parameters can be easily calculated from the provided information. The collector height (4 lines of PV modules) is 3.968 m. The normalized width is then $W/l = 8.266$. While the PV plant length is a priori unknown, we can approximate the plant aspect ratio considering the total length of available land: $W/L = 1.262$. The DC loss coefficient is set to $L_{DC} = 0.1$, which can be representative of a typical PV plant, while the AC loss coefficient is set to $L_{AC} = 0.04$ considering the losses in AC wires and power transformer. The peak power-related cost is calculated by the sum of PV

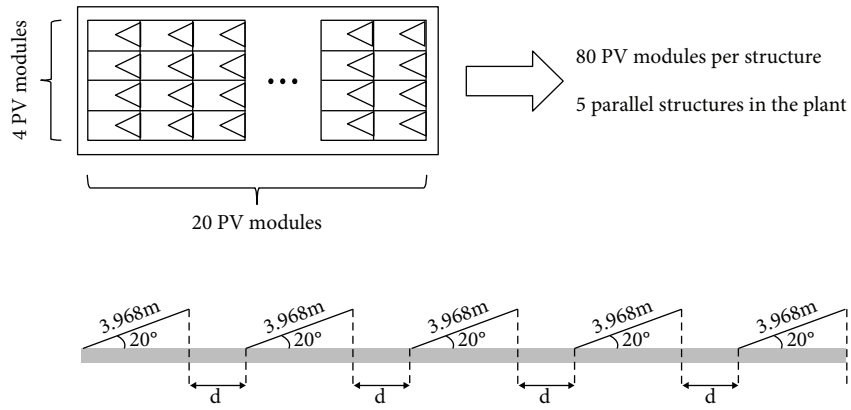

Figure 8: PV array structure and geometry of the example of application.

Table 3: Information required by the proposed optimization method for the example of application.

Source	Information
PV module datasheet	Max. power = 260 Wp
	Temp. coefficient = 0.40%/K
	NOCT = 45°C
	Module efficiency = 16.0%
	Module width = 0.992 m
	Module length = 1.690 m
Land geometry	Length = 26.0 m
	Width = 32.8 m
	Orientation = south-oriented
	Land tilt = horizontal
Preliminary design	Module tilt = 20°
	Number of mounting structures = 5
	Structure width = 32.8 m
	Structure collector height = 3.968 m
	Number of PV modules per structure = 80
	Total number of PV modules = 400
	Total peak power = 104,000 Wp
	Inverter nominal capacity = 17,000 W
	Number of inverters = 5
	AC nominal output power = 85,000 W
Budget	Cost per PV module = 134.20 USD
	Cost per inverter = 4210 USD
	Cost per structure = 3950 USD
	Cost of electrical protections = 12,421 USD
	Transformer cost = 1842 USD
	Manual labor cost = 4210 USD
	Building cost = 15,789 USD
	Wiring cost = 6856 USD
	Land cost = 4 USD/m^2

modules, PV inverters, electrical protections, transformer, manual labor, and building costs divided by the total PV plant peak power, $C_{kWp} = 1047$ USD/kWp. The cost per m^2 structure is $C_{m2str} = 30.35$ USD/m^2. The total wiring cost divided by the area of available land is 6.74 USD/m^2. If we sum the cost of the land, C_{m2land} results in 10.74 USD/m^2.

With these input parameters, the optimum free distance between rows of PV modules (d) can be calculated with the proposed method. Results are presented in Table 4. For comparison purposes, we have also calculated d by using two existing methods: one is the standard winter solstice rule as described in Section 4; the other is the method proposed by Novas-Castellano et al. [6], which calculates the exact shading shape on the land over 21st of December. The lowest value of occupied land area is obtained with the proposed methodology (799.4 m^2), followed by the winter solstice rule (812.7 m^2) and the method of Novas-Castellano et al. (851.0 m^2). This means that when land-related costs are considered in the analysis as in the case of the proposed method, the d distance tends to be lower. The other two methods are only based on shading irradiance calculations and do not consider this kind of information. As can be seen in the table, the differences in the energy yield are small in spite of the difference in the d distance. However, the economical objective function is impacted by the occupied land area, ranging from 1.2764 kWh/USD for the proposed method to 1.2737 kWh/USD for the method of Novas-Castellano et al. As a conclusion, this example shows the economic benefits of using the proposed method.

7. Conclusions

A methodology for optimizing the array spacing in grid-connected PV systems has been proposed. It uses annual shading energy calculations, an energy yield model of the PV system, and an economic approach based on the system investment costs. In this way, the method takes into consideration a number of technical and economic parameters that impact the optimum array spacing. It has been applied to the climate of Aguascalientes, Mexico, by using real atmospheric measurements registered over 10 years. However, the methodology can be easily applied to other locations with available climate data.

Table 4: Comparison between the proposed method, the standard winter solstice rule, and the method of Novas-Castellano et al. [6] for the calculation of the free distance between rows of PV modules (d).

Method	d (m)	Occupied land area (m^2)	Annual energy yield (kWh/kWp)	Objective function (kWh/USD)
This study	1.432	799.4	1690	1.2764
Winter solstice rule	1.533	812.7	1692	1.2761
Method of Novas-Castellano et al. [6]	1.825	851.0	1695	1.2737

The results have been compared to a common rule used by PV designers based on the winter solstice condition. While the simplified rule provides a unique value for the row-to-row distance for a given tilt, orientation, and location, the proposed methodology adapts to different parameters. For instance, considering south-oriented 20°-tilted PV modules, the free distance between rows normalized to the collector height can vary between 0.30 and 0.44 as a function of the land-related costs, compared to the fixed value of 0.38 obtained by the winter solstice rule. Therefore, the proposed method is more flexible and can be adapted to any specific project, improving its profitability.

When dealing with optimum array spacing, it is convenient to consider the minimum distance required for maintenance purposes. It is possible that the optimum free distance between rows is not sufficient for maintenance. Our recommendation in this case is to increase the collector height if possible, for instance, by adding an additional line of PV modules or installing the PV modules with the longest side in vertical. In this way, the optimum distance will increase and allow the maintenance activities. In the case that esthetical or structural limitations avoid implementing these adjustments, then the optimum distance could not be used, although this will imply economic losses because of the higher amount of occupied land due to a longer free distance between rows.

The methodology can be used as a framework to analyze the impact of each individual technical or economic parameter on the optimum array spacing. Results of a sensibility analysis have allowed sorting the involved parameters as a function of their impact. Considering technical parameters, the main relevant factors are the module tilt ($\Delta d/l = 94.89\%$), the ratio of plant width to plant length ($\Delta d/l = 15.14\%$), and the PV module efficiency ($\Delta d/l = 8.45\%$), while considering economic parameters, the main relevant factors are the land-related costs ($\Delta d/l = 32.98\%$) and the cost per kWp ($\Delta d/l = 7.94\%$). These results can help the PV designer in the selection of the system components and geometry. There was a lack in the reviewed literature concerning this kind of analysis. The methodology is analytical and easy to use, facilitating its usage in real PV projects.

Future work will incorporate more complex economic methodologies such as the LCOE, PV systems installed on a nonhorizontal land, and sun-tracking systems.

Data Availability

The meteorological data used to support the findings of this study have not been made available because they belong to Coordinación General del Servicio Meteorológico Nacional (CGSMN) of the Comisión Nacional del Agua (CONAGUA) of México.

Conflicts of Interest

The authors declare that there is no conflict of interests regarding the publication of this paper.

Acknowledgments

The authors thank the Coordinación General del Servicio Meteorológico Nacional (CGSMN) of the Comisión Nacional del Agua (CONAGUA) of México because of the supply of the meteorological data used in this research. Pedro M. Rodrigo thanks the Science and Technology National Council of Mexico (CONACYT) for the economic support as a member of the National System of Researchers.

References

[1] P. P. Groumpos and K. Khouzam, "A generic approach to the shadow effect of large solar power systems," *Solar Cells*, vol. 22, no. 1, pp. 29–46, 1987.

[2] M. M. Elsayed and A. M. al-Turki, "Calculation of shading factor for a collector field," *Solar Energy*, vol. 47, no. 6, pp. 413–424, 1991.

[3] J. Appelbaum and J. Bany, "Shadow effect of adjacent solar collectors in large scale systems," *Solar Energy*, vol. 23, no. 6, pp. 497–507, 1979.

[4] S. B. Sadineri, R. F. Boehm, and R. Hurt, "Spacing analysis of an inclined solar collector field," in *ASME 2nd International Conference on Energy Sustainability*, pp. 417–422, Jacksonville, FL, USA, 2008.

[5] D. Weinstock and J. Appelbaum, "Optimal solar field design of stationary collectors," *Journal of Solar Energy Engineering*, vol. 126, no. 3, pp. 898–905, 2004.

[6] N. N. Castellano, J. A. Gázquez Parra, J. Valls-Guirado, and F. Manzano-Agugliaro, "Optimal displacement of photovoltaic array's rows using a novel shading model," *Applied Energy*, vol. 144, pp. 1–9, 2015.

[7] J. K. Copper, A. B. Sproul, and A. G. Bruce, "A method to calculate array spacing and potential system size of photovoltaic arrays in the urban environment using vector analysis," *Applied Energy*, vol. 161, no. 1, pp. 11–23, 2016.

[8] Australian Photovoltaic Institute, *Solar Potential Tool*, Australian Renewable Energy Agency, 2014, http://pv-map.apvi.org.au/potential.

[9] D. Weinstock and J. Appelbaum, "Optimization of solar photovoltaic fields," *Journal of Solar Energy Engineering*, vol. 131, no. 3, article 031003, 2009.

[10] H. Awad, M. Gul, C. Ritter et al., "Solar photovoltaic optimization for commercial flat rooftops in cold regions," in *2016 IEEE Conference on Technologies for Sustainability (SusTech)*, Phoenix, AZ, USA, 2016.

[11] A. Martinez-Rubio, F. Sanz-Adan, and J. Santamaria, "Optimal design of photovoltaic energy collectors with mutual shading for pre-existing building roofs," *Renewable Energy*, vol. 78, pp. 666–678, 2015.

[12] M. Iqbal, *An Introduction to Solar Radiation*, Academic Press, Toronto, Canada, 1983.

[13] P. M. Rodrigo, R. Velázquez, and E. F. Fernández, "DC/AC conversion efficiency of grid-connected photovoltaic inverters in central Mexico," *Solar Energy*, vol. 139, pp. 650–665, 2016.

[14] T. Maor and J. Appelbaum, "View factors of photovoltaic collector systems," *Solar Energy*, vol. 86, no. 6, pp. 1701–1708, 2012.

[15] S. Gutiérrez and P. M. Rodrigo, "Energetic analysis of simplified 2-position and 3-position North-South horizontal single-axis sun tracking concepts," *Solar Energy*, vol. 157, pp. 244–250, 2017.

[16] C. Rus-Casas, J. D. Aguilar, P. Rodrigo, F. Almonacid, and P. J. Pérez-Higueras, "Classification of methods for annual energy harvesting calculations of photovoltaic generators," *Energy Conversion and Management*, vol. 78, pp. 527–536, 2014.

[17] International Electrotechnical Commission (IEC), *IEC 61853–1: Photovoltaic (PV) Module Performance Testing and Energy Rating - Part 1: Irradiance and Temperature Performance Measurements and Power Rating*, Geneva, Switzerland, 2011.

[18] B. Bletterie, R. Bründlinger, and G. Lauss, "On the characterisation of PV inverters' efficiency - introduction to the concept of achievable efficiency," *Progress in Photovoltaics: Research and Applications*, vol. 19, no. 4, pp. 423–435, 2011.

[19] K. Peippo and P. D. Lund, "Optimal sizing of solar array and inverter in grid-connected photovoltaic systems," *Solar Energy Materials and Solar Cells*, vol. 32, no. 1, pp. 95–114, 1994.

[20] P. J. Pérez-Higueras, F. M. Almonacid, P. M. Rodrigo, and E. F. Fernández, "Optimum sizing of the inverter for maximizing the energy yield in state-of-the-art high-concentrator photovoltaic systems," *Solar Energy*, vol. 171, pp. 728–739, 2018.

[21] P. M. Rodrigo, "Improving the profitability of grid-connected photovoltaic systems by sizing optimization," in *2017 IEEE Mexican Humanitarian Technology Conference (MHTC)*, Puebla, Mexico, 2017.

[22] J. C. Lagarias, J. A. Reeds, M. H. Wright, and P. E. Wright, "Convergence properties of the Nelder-Mead simplex method in low dimensions," *SIAM Journal on Optimization*, vol. 9, no. 1, pp. 112–147, 1998.